Available online at www.sciencedirect.com

ScienceDirect

Nuclear Physics B 964 (2021) 115304

NUCLEAR PHYSICS B

www.elsevier.com/locate/nuclphysb

Studying the neutrino wave-packet effects at medium-baseline reactor neutrino oscillation experiments and the potential benefits of an extra detector

Zhaokan Cheng [a,*], Wei Wang [b,c,*], Chan Fai Wong [b], Jingbo Zhang [a]

[a] *School of Physics, Harbin Institute of Technology, Harbin, China*
[b] *School of Physics, Sun Yat-sen University, GuangZhou, China*
[c] *Sino-French Institute of Nuclear Engineering and Technology, Sun Yat-sen University, Zhuhai, China*

Received 28 September 2020; received in revised form 29 December 2020; accepted 30 December 2020
Available online 27 January 2021
Editor: Tommy Ohlsson

Abstract

We examine the potential of the future medium-baseline reactor neutrino oscillation (MBRO) experiments in studying neutrino wave-packet impact. In our study, we treat neutrinos as wave packets and use the corresponding neutrino flavor transition probabilities. The delocalization, separation and spreading of the wave packets lead to decoherence and dispersion effects, which modify the plane-wave neutrino oscillation pattern, by amounts that depend on the energy uncertainties in the initial neutrino wave packets. We find that MBRO experiments could be sensitive to the wave-packet impact, since the baseline is long enough and also the capability of observing small corrections to the neutrino oscillations due to excellent detector energy resolution. Besides studying the constraints on the decoherence parameter, we also examine the potential wave-packet impacts on the precision of measuring θ_{12} and other oscillation parameters in the future medium-baseline reactor neutrino oscillation experiments. Moreover, we also probe the potential benefits of an additional detector for studying such exotic neutrino physics.

* Corresponding authors.
E-mail addresses: 14B911018@hit.edu.cn (Z. Cheng), wangw223@mail.sysu.edu.cn (W. Wang), huangzhh58@mail.sysu.edu.cn (C.F. Wong), jinux@hit.edu.cn (J. Zhang).

https://doi.org/10.1016/j.nuclphysb.2021.115304

1. Introduction

The plane-wave description of neutrino mixing and oscillation has been the standard picture for neutrino oscillation [1] and all the parameters have been defined and analyzed based on such a picture. Till now, this standard picture has been very consistent with the neutrino experimental data [2,3]. However, as neutrino production and detection are spatially localized, there must be finite intrinsic energy/momentum uncertainties. A wave-packet description is naturally expected to be more general and appropriate for a complete understanding of neutrino oscillations in reality [2–10]. As neutrino physics is entering a precision stage, more advanced detector technologies are becoming available, especially the MBRO type experiments of resolving neutrino mass ordering (MO) [11–20], which is made possible by an unexpectedly large value of θ_{13} found by the current generation of short-baseline reactor neutrino and long-baseline accelerator neutrino experiments [21–25].

Due to the capability of measuring the multiple oscillation cycles, MBRO detectors are expected to be also sensitive to potential damping signatures resulted from various non-standard mechanisms of neutrino flavour transitions, such as the neutrino wave-packet hypothesis [2,3,8,9,26–34]. Particularly, references [2,32] mention that the decoherence effect could be significant /measurable in medium baseline (around 50 km) reactor neutrino experiment(s). As the first MBRO project, the JUNO experiment consists of a large central detector with unprecedented energy resolution ($3\%/\sqrt{E/\mathrm{MeV}}$), a water Cherenkov detector and a muon tracker. The central detector is a liquid scintillator (LS) detector within a target mass of 20 kton at a spherical container of ~ 35.4 m diameter. It is built in the Jinji town located at ~ 52.5 km from the Yangjiang Nuclear Power Plant (NPP) and Taishan NPP, where 10 rector cores offer a combined thermal power of $\sim 35.8\ \mathrm{GW_{th}}$. With such a setup, the JUNO experiment is believed to be a state-of-the-art platform to identify the neutrino mass ordering and also perform the precision measurements of various neutrino oscillation parameters, such as θ_{12}, Δm^2_{21} and Δm^2_{ee} [20]. In the following, we will also discuss the wave-packet impact on such precision measurements.

In this article, we apply a wave-packet treatment to neutrino oscillations and probe the potential of MBRO experiments in studying the neutrino wave-packet hypothesis. We examine the constraints on the decoherence parameter (σ_{wp}) at medium-baseline reactor neutrino oscillation experiments and also investigate how does the neutrino wave-packet treatment affect the precision measurement of oscillation parameters. This article is organized as follows. In section 2, we discuss the mechanism of neutrino wave-packet treatment and briefly review the discussions in the literature about this hypothesis. In section 3, we show the resulting constraints on the neutrino wave-packet parameter from the future MBRO experiment(s) and compare them with the current constraints from Daya Bay. Then in section 4, we discuss the wave-packet impacts on the precision measurement of oscillation parameters. In section 5, we further discuss the potential of an extra detector at MBRO experiment(s) on the studies of decoherence and dispersion effects due to neutrino wave-packet treatment. At last, a summary of our results and perspectives are presented in section 6.

2. The neutrino wave-packet hypothesis

The plane-wave description of neutrino oscillation has been developed for almost 40 years [1]. However, as neutrino production and detection are spatially localized, there must be finite intrinsic energy/momentum uncertainties and a neutrino should be described by a wave packet. A wave-packet description is expected to be more general and appropriate for a complete under-

standing of neutrino oscillations in reality, each neutrino emitted from the source should have a mixture of energy/momentum states, and thus a wave-packet (WP) description is more self-consistent and appropriate, which leads to modification of the plane-wave neutrino oscillation probability by terms that depend on the energy/momentum width of the initial neutrino wave packet, σ_ν [2–10]. Massive neutrino should be described by a wave packet as it propagates freely [5,9,10]:

$$|\nu_i(z,t)\rangle = \int_{-\infty}^{\infty} \frac{dp}{\sqrt{2\pi}} \frac{1}{\sqrt{\sqrt{\pi}\sigma_\nu}} \exp\left[-\frac{(p-p_\nu)^2}{2\sigma_\nu^2}\right] \cdot \exp\left[i\,(pz - E_i(p)t)\right] |\nu_i\rangle, \tag{1}$$

$$|\nu_\alpha(z,t)\rangle = \sum_i U_{\alpha i}^* |\nu_i(z,t)\rangle, \tag{2}$$

where $|\nu_i\rangle$ is an energy eigenstate with energy E_i, p_ν is the mean momentum, σ_ν is the width of the wave packet in momentum space,[1] assumed to be independent of the neutrino energy here, and $|\nu_\alpha\rangle$ is a neutrino flavor state.

2.1. The conventional decoherence effect due to separation of wave packets

In order to calculate the integral in Eq. (1), the energy $E_i(p)$ has to be expanded around the mean momentum p_ν. In most decoherence literatures, it is just expanded to first order as the higher order terms are expected to be strongly suppressed by the factors of $(\frac{m^2}{E_i^2})^n$:

$$E_i(p) \approx E_i(p_\nu) + v_i(p_\nu)(p - p_\nu), \tag{3}$$

where $v_i(p_\nu) = \left.\frac{dE_i}{dp}\right|_{p=p_\nu} = p_\nu/E_i(p_\nu)$, which is the group velocity of the wave packet. Based on Eqs. (1) and (3), the neutrino oscillation probability of $\nu_\alpha \to \nu_\beta$ would be given by [36]:

$$P_{\nu_\alpha\to\nu_\beta}(L) \approx \sum_{ij}\left[U_{\alpha i}^* U_{\beta i} U_{\alpha j} U_{\beta j}^* \exp\left(-i\frac{2\pi L}{L_{ij}^{\rm osc}}\right)\right] \exp\left(-\frac{L^2}{(L_{ij}^{\rm coh})^2}\right) \tag{4}$$

$$\text{where } L_{ij}^{\rm osc} \equiv \frac{4\pi E}{\Delta m_{ij}^2}, \qquad L_{ij}^{\rm coh} \equiv \frac{L_{ij}^{\rm osc}}{\pi\sigma_{\rm wp}} = \frac{4E}{\Delta m_{ij}^2 \sigma_{\rm wp}}, \qquad \sigma_{\rm wp} \equiv \frac{\sigma_\nu}{E_i(p_\nu)} \approx \frac{\sigma_\nu}{E(p_\nu)}.$$

$L_{\rm coh}$ is the coherence length, which represents the distance where the decoherence effect becomes significant.

In the future medium-baseline reactor neutrino oscillation experiment(s), the $\bar{\nu}_e$ survival probability formula would be rewritten as

[1] Here, σ_ν is the effective uncertainty, with $1/\sigma_\nu^2 = 1/\sigma_{\rm prod}^2 + 1/\sigma_{\rm det}^2$, which has included both the production and detection neutrino energy uncertainties [6,26,35]. Moreover, we would like to point out that $\sigma_{\rm det}$ represents the energy uncertainty of detection at the microscopic level, i.e., that of the inverse-beta decay reaction. This is different from the detector energy resolution, which is determined by macroscopic parameters such as the performance of PMTs and geometry of the anti-neutrino detector, etc. In principle, the detector resolution is irrelevant for the size of the neutrino wave packets.

$$
\begin{aligned}
P_{\bar{e}\bar{e}} = 1 &- \frac{1}{2}\cos^4(\theta_{13})\sin^2(2\theta_{12})\left[1-\exp\left(-\sigma_{\rm wp}^2\frac{(\Delta m^2_{21})^2L^2}{16E^2}\right)\cos\left(2\frac{\Delta m^2_{21}L}{4E}\right)\right] \\
&- \frac{1}{2}\sin^2(2\theta_{13})\cos^2(\theta_{12})\left[1-\exp\left(-\sigma_{\rm wp}^2\frac{(\Delta m^2_{31})^2L^2}{16E^2}\right)\cos\left(2\frac{\Delta m^2_{31}L}{4E}\right)\right] \\
&- \frac{1}{2}\sin^2(2\theta_{13})\sin^2(\theta_{12}) \\
&\times\left[1-\exp\left(-\sigma_{\rm wp}^2\frac{(|\Delta m^2_{31}|-\Delta m^2_{21})^2L^2}{16E^2}\right)\cos\left(2\frac{(|\Delta m^2_{31}|-\Delta m^2_{21})L}{4E}\right)\right]. \qquad (5)
\end{aligned}
$$

Eqs. (4) and (5) could be found in most decoherence literatures [27,36,37], which describe the decoherence effect due to the fact that different mass eigenstates travel with different speeds and they therefore gradually separate, reducing their interference and leading to a damping of neutrino oscillations. However, the quadratic correction to the neutrino energy and the decoherence effect due to delocalization (i.e., the spatial width of neutrino wave packet σ_x being too large) [2,26] have not been taken into account yet. In the following subsection, we will derive the oscillation probability more precisely.

2.2. *The dispersion effect*

In this subsection, we use the wave-packet treatment and approximations in Reference [2] to calculate the integral in Eq. (1), which includes the second order correction to the neutrino energy.

$$
E_i(p) \approx E_i(p_\nu) + v_i(p_\nu)(p-p_\nu) + \frac{m_i^2}{2(E_i(p_\nu))^3}(p-p_\nu)^2. \qquad (6)
$$

Conventionally, the last term in Eq. (6) is neglected since it is strongly suppressed by the factor $(\frac{m_i^2}{E_i^2})$. However, this term give rises to the dispersion of the wave packet and would alter the survival probability if $\sigma_{\rm wp}$ is large. The phenomenological consequence of this term is that the dispersion effect will partially compensate the decoherence effect due to the linear term in Eq. (6) and further modify the neutrino oscillation pattern. Then the neutrino flavor transition probabilities at baseline L is given by:

$$
\begin{aligned}
P_{\nu_\alpha\to\nu_\beta}(L) \approx \sum_{ij}&\left\{U^*_{\alpha i}U_{\beta i}U_{\alpha j}U^*_{\beta j}\exp\left[-i\frac{2\pi L}{L^{\rm osc}_{ij}}\right]\right\} \\
&\left\{\left(\frac{1}{1+\epsilon_{ij}^2}\right)^{\frac{1}{4}}\exp(-\Gamma_{ij})\exp\left[\frac{-i}{2}\tan^{-1}(\epsilon_{ij})\right]\exp(i\Gamma_{ij}\epsilon_{ij})\right\}, \qquad (7)
\end{aligned}
$$

$$
\text{where } \Gamma_{ij}\equiv\frac{\eta_{ij}^2}{1+\epsilon_{ij}^2}, \qquad \epsilon_{ij}\equiv\frac{L}{L^{\rm dis}_{ij}}, \qquad \eta_{ij}\equiv\frac{L}{L^{\rm coh}_{ij}},
$$

$$
L^{\rm osc}_{ij}\equiv\frac{4\pi E}{\Delta m^2_{ij}}, \qquad L^{\rm coh}_{ij}\equiv\frac{4E}{\Delta m^2_{ij}\sigma_{\rm wp}}, \qquad L^{\rm dis}_{ij}\equiv\frac{2E}{\Delta m^2_{ij}\sigma^2_{\rm wp}},
$$

$$\sigma_{\rm wp} = \frac{\sigma_v}{E_i(p_v)} \approx \frac{\sigma_v}{E(p_v)}.$$

The terms in the first bracket correspond to the standard plane-wave oscillation probabilities, and those in the second bracket represent the modifications due to wave-packet impact. The $\exp(-\Gamma_{ij})$ term corresponds to the decoherence effect due to the fact that different mass states propagate at different speeds $v_i(p_v)$ and they gradually separate and stop to interfere with each other, resulting in a damping of oscillations. The terms depending on ϵ_{ij} describe the dispersion effects and are dependent of the dispersion length(s) $L_{ij}^{\rm dis}$. Furthermore, ϵ_{ij} are proportional to $\sigma_{\rm wp}^2$, while $\eta_{ij} \propto \sigma_{\rm wp}$ only. Therefore, if $\sigma_{\rm wp} \ll 1$, the dispersion effect is expected to be more suppressed and negligible. Dispersion has two effects on the oscillations. On the one hand, the spreading of the wave packet compensates for the spatial separation of the mass states, hence restoring parts of their interferences. On the other hand, dispersion reduces the overlapping fraction of the wave packets, and thus the interference or oscillation effects cannot be fully restored. Moreover, it also modifies the flavor oscillation phases:

$$\phi_{ij} \equiv \frac{2\pi L}{L_{ij}^{\rm osc}} + \left[\frac{1}{2}\tan^{-1}(\epsilon_{ij}) - \Gamma_{ij}\epsilon_{ij}\right], \tag{8}$$

with deviations from the standard plane-wave oscillation phase written in the parentheses. If $\epsilon_{ij} = 0$, then ϕ_{ij} just reduce to the standard plane-wave oscillation phases.

2.3. Decoherence effect due to delocalization

The decoherence effect mentioned in the previous subsection is due to the separation of different neutrino wave packets. With larger values of $\sigma_{\rm wp}$, the corresponding decoherence effect would be more significant. On the other hand, there also exists another kind of decoherence effect not described in the previous subsections, due to the delocalization of the production and detection processes. Different with what we have studied above, the decoherence effect from delocalization[2] will become significant only when $\sigma_{\rm wp}$ is extremely small.

An extremely small value of $\sigma_{\rm wp}$ implies a large spatial width of the wave packet (σ_x), which will lead to the other kind of damping signature of the neutrino oscillations. With these delocalization terms taken into account, a more complete $\bar{\nu}_e$ survival probability is given by[3]:

$$P_{\nu_\alpha\to\nu_\beta}(L) \approx \sum_{ij}\left\{U_{\alpha i}^* U_{\beta i} U_{\alpha j} U_{\beta j}^* \exp\left[-i\frac{\Delta m_{ij}^2 L}{2E}\right]\right\}$$
$$\left\{\left(\frac{1}{1+\epsilon_{ij}^2}\right)^{\frac{1}{4}} \exp(-\Gamma_{ij})\exp\left[\frac{-i}{2}\tan^{-1}(\epsilon_{ij})\right]\exp(i\Gamma_{ij}\epsilon_{ij})\right\}\exp(-\gamma_{ij}), \tag{9}$$

$$\text{where } \gamma_{ij} = \frac{\frac{1}{16}\frac{(\Delta m_{ij}^2)^2}{E^4}}{1+\epsilon_{ij}^2}\cdot\frac{1}{\sigma_{\rm wp}^2} = \frac{\pi^2}{(1+\epsilon_{ij}^2)}\cdot\frac{\sigma_x^2}{(L_{ij}^{\rm osc})^2}.$$

[2] In the following content, we will call this kind of decoherence effect as delocalization effect in order to separate it from the decoherence effect due to separation of wave packets.

[3] The details of the derivation of oscillation formula can be found in reference [2].

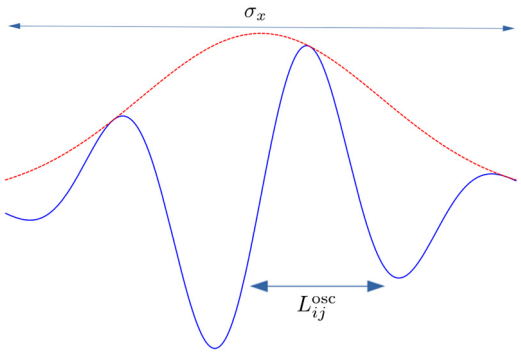

Fig. 1. Schematic representation of the decoherence effects due to the delocalization term in Eq. (9). When the width of wave packet is comparable or even larger than the oscillation length, the oscillation would be destroyed.

The additional damping factor exp(-γ_{ij}) is important when σ_x becomes comparable to $L_{ij}^{\rm osc}$. In the previous subsections, we have assumed the terms $\propto \frac{\frac{(\Delta m_{ij}^2)^2}{E^4}}{\sigma_{\rm wp}^2}$ are negligible since they are inversely proportional to $\sigma_{\rm wp}^2$, which will be significant only if $\sigma_{\rm wp} \lesssim O(10^{-16})$. Fig. 1 further describes the extreme case when $\sigma_x \gg L_{ij}^{\rm osc}$; in such circumstances it is difficult to observe the oscillation effect.

In fact, in neutrino oscillation, one of the coherence conditions is that the intrinsic production (and also detection) energy uncertainties are much larger than the energy difference between different mass eigenstates (ΔE_{ij}) [38], namely,

$$\Delta E_{ij} \equiv E_i - E_j \sim \frac{\Delta m_{ij}^2}{E_\nu} \ll \sigma_\nu \equiv E_\nu \sigma_{\rm wp}. \tag{10}$$

Eq. (10) implies that in order to measure the interferences between different mass eigenstates, the spatial uncertainty σ_x has to be much smaller than the oscillation length. Namely, $\sigma_x \ll L_{\rm osc}$.

The condition in Eq. (10) is satisfied in most reactor neutrino oscillation measurements, since the production and detection processes are (spatially) localized in regions smaller than the reactor and detector sizes, which are much smaller than the oscillation length.[4] Therefore, in most of the neutrino oscillation experiments,

$$\gamma_{ij} = \frac{\pi^2}{(1+\epsilon_{ij}^2)} \cdot \frac{\sigma_x^2}{(L_{ij}^{\rm osc})^2} \approx 0. \tag{11}$$

Thus, in most circumstances, the delocalization damping term $\exp(-\gamma_{ij})$ can be safely neglected.

It is obvious that in Eq. (9), the terms of γ_{ij} do not allow $\sigma_{\rm wp}$ to go to zero as $\gamma_{ij} \propto 1/\sigma_{\rm wp}$. The decoherence effect due to delocalization would lead to a lower bound of the possible range of $\sigma_{\rm wp}$. On the other hand, the terms of Γ_{ij} and ϵ_{ij} are significant only when $\sigma_{\rm wp}$ is large. This implies that if $\sigma_{\rm wp}$ is extremely small, the decoherence due to spatial separations is negligible

[4] However, in the measurement of sterile neutrino oscillation, the oscillation length is expected to be short and may be comparable to the spatial uncertainty σ_x. In this case the decoherence effect coming from the localization term should not be neglected.

and even dispersion effect is also subdominant. Γ_{ij} and ϵ_{ij} would lead to the upper limit of the allowed region of $\sigma_{\rm wp}$. In a word, in the wave-packet treatment, only one extra parameter is introduced ($\sigma_{\rm wp}$ or σ_v) but it can describe two different decoherence effects. It is because the energy uncertainty ($\sigma_{\rm wp}$) being either too large or too small[5] would also destroy the oscillation. Both the separation of wave packets and the delocalization effect depend on the initial width of the neutrino wave packet.

2.4. The estimation of $\sigma_{\rm wp}$

The value of this parameter or the size of neutrino wave packet has not come to a strong conclusion yet. Up to now, Daya Bay is the only neutrino experiment which provides the experimental constraints [3] on this parameter. Besides, references [2,34] provide experimental bounds on the $\sigma_{\rm wp}$ (or σ_x) based on the data from Daya Bay and other reactor neutrino experiments. On the other hand, there have been different theoretical estimations of the sizes of neutrino wave packets produced in different situations. For example, Reference [39] uses the pion decay length to estimate the width of neutrino wave packet in the MINOS experiment and argues that there could be significant decoherence effect in the active to sterile neutrino oscillation in MINOS.[6] Regarding to reactor neutrino experiments, Reference [37] provides an estimation based on the mean free path and mean thermal velocity of the production process and suggests that $\sigma_x \sim 10^{-6}$ m, which implies that $\sigma_{\rm wp} \sim 10^{-7}$ in reactor neutrino experiments. Meanwhile, References [40,41] suggest that the neutrino emission process is expected to be localized at the scale of interatomic distance, and so $\sigma_x \lesssim 10^{-10}$ m, implying $\sigma_{\rm wp} \sim 10^{-3}$ or even larger. If on the other hand, one takes the uncertainty of a nucleon's position in a nucleus as σ_x, then $\sigma_{\rm wp}$ could be much larger, even of order 1. The estimated sizes of neutrino wave packets from different approaches could be different by a few orders of magnitude. Moreover, as pointed out by Reference [26], the relation between the decay time of the source and the wave packet size of the oscillating particle is not direct. The decay time only puts an upper bound on the wave packet length. Such estimations are within the experimental bounds from references [2,3,34], but there are no solid support for such theoretical estimations yet.

2.5. The impact of $\sigma_{\rm wp}$ on oscillation probability

As the MBRO experiment(s) is designed to detect electron anti-neutrinos via the inverse beta decay (IBD): $\bar{\nu}_e + p \to e^+ + p$, we focus on the $\bar{\nu}_e$ survival probability:

$$P_{\bar{e}\bar{e}} = 1 - \frac{1}{2}\cos^4(\theta_{13})\sin^2(2\theta_{12})\left[1 - \left(\frac{1}{1+\epsilon_{21}^2}\right)^{\frac{1}{4}} \cdot \exp(-\Gamma_{21})\exp(-\gamma_{21})\cos(\phi_{21})\right]$$
$$- \frac{1}{2}\sin^2(2\theta_{13})\cos^2(\theta_{12})\left[1 - \left(\frac{1}{1+\epsilon_{31}^2}\right)^{\frac{1}{4}} \cdot \exp(-\Gamma_{31})\exp(-\gamma_{31})\cos(\phi_{31})\right]$$

[5] Small energy uncertainty implies large spatial uncertainty.

[6] Please notice that the decoherence effect in Reference [39] is due to the delocalization, different with the decoherence effect due to separations of wave packets but it could also destroy the oscillation.

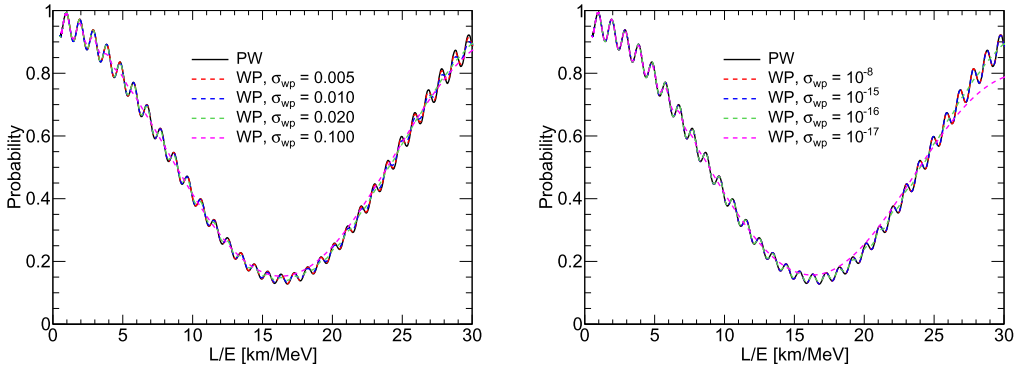

Fig. 2. $P_{\bar{e}\bar{e}}$ as a function of L/E for MBRO (L = 53 km) under different assumptions of $\sigma_{\rm wp}$. The left panel corresponds to the assumptions of relatively large $\sigma_{\rm wp}$, and the right panel shows the comparisons of extremely small $\sigma_{\rm wp}$. In both panels, the black solid curves are the standard plane-wave result.

$$-\frac{1}{2}\sin^2(2\theta_{13})\sin^2(\theta_{12})\left[1-\left(\frac{1}{1+\epsilon_{32}^2}\right)^{\frac{1}{4}}\cdot\exp(-\Gamma_{32})\exp(-\gamma_{32})\cos(\phi_{32})\right]. \tag{12}$$

The oscillation parameter values are taken from global analysis [42] as $\Delta m^2_{21} = 7.53 \times 10^{-5}$ eV^2, $(\Delta m^2_{31} + \Delta m^2_{32})$ / 2 = 2.548×10^{-3} eV^2, $\sin^2\theta_{12} = 0.307$ and $\sin^2\theta_{13} = 0.0212$. The neutrino wave-packet impact on the oscillation curves is shown in Fig. 2.

In Fig. 2, we use Eq. (12) to calculate the $\bar{\nu}_e$ survival probability with different $\sigma_{\rm wp}$ values. Meanwhile, we also extract the $\bar{\nu}_e$ survival probability from the standard plane-wave oscillation formula. For large and small $\sigma_{\rm wp}$, the probabilities are shown in the left and the right panels of Fig. 2, respectively. Basically, the oscillation probability of wave-packet framework is approximated to be same with the one of plane-wave framework if $\sigma_{\rm wp}$ is within the range from 10^{-15} to 0.005. If $\sigma_{\rm wp}$ is larger than 0.01 or smaller than 10^{-16}, the probability of wave-packet framework would gradually deviate from the one of plane-wave framework.

3. The constraints from medium-baseline reactor neutrino oscillation experiment

Thus far, there are no significant signals of decoherence and dispersion effects caused by the neutrino wave-packet treatment. The Daya Bay collaboration have analyzed their data with the neutrino wave-packet framework and managed to provide lower and upper limits on the value of $\sigma_{\rm wp}$[7]: $2.38 \times 10^{-17} < \sigma_{\rm rel} < 0.23$ at 95% C.L. [3]. In view of this work, we use Eq. (12) to perform numerical simulations at the future medium baseline reactor experiment(s) and estimate its sensitivities on the constraints of $\sigma_{\rm wp}$.

We quantify the sensitivity of $\sigma_{\rm wp}$ by employing the least-squares method, based on a χ^2 function given by

[7] Please note that our definition of σ_v is different with the corresponding parameter σ_p in reference [3]: $\sigma_v = \sqrt{2}\sigma_p$. Therefore the value of $\sigma_{\rm wp}$ is also $\sqrt{2}$ times larger than the $\sigma_{\rm rel}$ in that paper.

$$\chi^2 = \sum_i^{N_{\rm bin}} \frac{[T_i - F_i(1+\eta_R+\eta_d+\eta_i)]^2}{T_i} + \left(\frac{\eta_R}{\sigma_R}\right)^2 + \left(\frac{\eta_d}{\sigma_d}\right)^2 + \sum_i^{N_{\rm bin}} \left(\frac{\eta_i}{\sigma_{s,i}}\right)^2 \tag{13}$$

where T_i is measured neutrino event in the ith energy bin, and F_i is the predicted number of neutrino events with oscillations taken into account (the fitting event rate). η with different subscripts are nuisance parameters corresponding to reactor-related uncertainty (σ_R), detector-related uncertainty (σ_d) and shape uncertainty (σ_s). According to the References [20,43,44], σ_R, σ_d and $\sigma_{s,i}$ are assumed to be 2%, 1% and 1% at MBRO experiment(s), respectively.

In numerical simulations, we set up the MBRO experiment(s) according to the JUNO experimental configurations: $3\%/\sqrt{E/\text{MeV}}$ energy resolution, $\sim$ 52.5 km baseline and $\sim$ 20 ktons target mass. For simplicity, we use one single $\sim$ 35.8 GW_{th} reactor core to alternate 10 reactor cores. Furthermore, we also adopt a 6 years running-time. To calculate T_i, we set the input value of $\sigma_{\rm wp}$ to be equal to 10^{-8} as this treatment won't cause the probability derivation between wave-packet and plane-wave frameworks as shown in the right panel of Fig. 2. With all the above setups, we attain the upper and lower limits on $\sigma_{\rm wp}$ and make a comparison with the results from Daya Bay. In addition, we change the running-time, shape uncertainties, energy resolutions and evaluate their impacts on the constraints to $\sigma_{\rm wp}$.

3.1. The upper and lower limits

If $\sigma_{\rm wp}$ is relatively large, in this case the decoherence effect is resulted from the separations of wave packets. Moreover, in this region, the dispersion effect could be significant and lead to modifications on the decoherence effect [2], which makes the oscillation patterns more complicated. The future MBRO experiment is expected to be sensitive to the decoherence and dispersion effects and provides constraint on decoherence parameter $\sigma_{\rm wp}$. The results of our simulations are correspondingly shown in the top panel of Fig. 3. The resulting upper bounds are found to be 0.0086, 0.0127, 0.0162 at 1, 2, 3 σ C.L., respectively.

On the other hand, if $\sigma_{\rm wp}$ is extremely small, which means that the spatial uncertainty of the neutrino wave packet is large, the delocalization will lead to the other kind of decoherence effect as the damping factor exp(-γ_{ij}) in Eq. (12). However, in the region of extremely small $\sigma_{\rm wp}$, the dispersion effect can be safely neglected. The results of the lower limit based on our numerical simulations are shown in the bottom panel of Fig. 3. The lower bounds are found to be 1.13×10^{-16}, 7.42×10^{-17}, 5.58×10^{-17} at 1, 2, 3 σ C.L. As discussed in the subsection 2.3, the decoherence effect due to delocalization is significant only when the spatial width of the neutrino wave packet (σ_x) is comparable to the oscillation length ($L^{\rm osc}$). Since the MBRO experiment(s) is expected to be able to observe both the atmospheric- and solar- Δm^2 driven oscillations, it is supposed to be sensitive to the delocalization effect in a large range. However, $L_{32}^{\rm osc} \sim O(1\text{km})$, $L_{21}^{\rm osc} \sim O(50\text{km})$. It means that σ_x has to be around a few hundred meters, otherwise the delocalization effect will be insignificant in the future MBRO experiment(s).

In fact, Fig. 3 shows that the lower limit of our simulation is around $\sigma_{\rm wp} \sim O(10^{-16})$, which corresponds to $\sigma_x \sim O(1\text{km})$. Nevertheless, it is obvious that the spatial width of the neutrino wave packet should not be larger than the dimensions of the reactor cores and detectors, which are just around $O(10)$ meters. Therefore, we conclude that the future MBRO experiment(s) cannot provide a stringent lower bound to $\sigma_{\rm wp}$. In the following sections, we will focus on the studies of upper bound and neglect the decoherence effect due to delocalization.

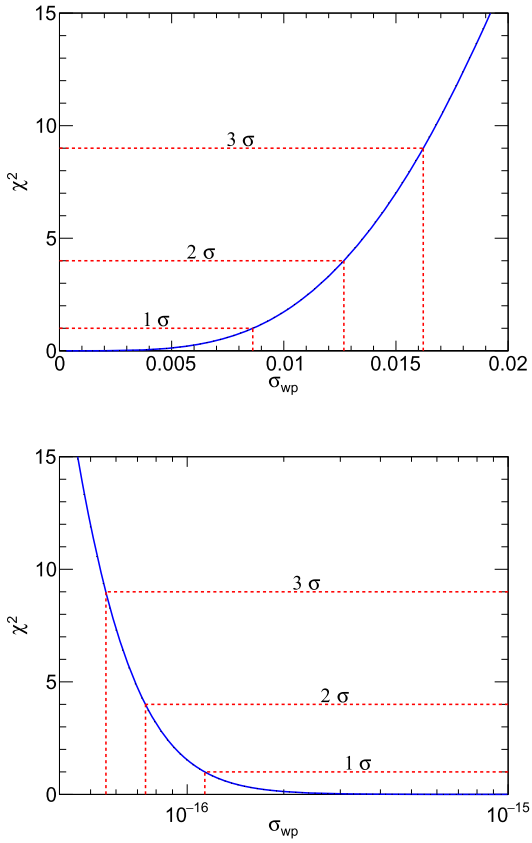

Fig. 3. Top: the 1, 2, 3 σ C.L. upper bound on $\sigma_{\rm wp}$ at the future medium-baseline reactor neutrino oscillation experiment(s). Bottom: the 1, 2, 3 σ C.L. lower bound on $\sigma_{\rm wp}$.

3.2. The impacts of statistical, shape uncertainties and detector energy resolutions on the sensitivity

The sensitivities in Fig. 3 corresponds to the assumption of 6 years data-taking and 1% shape uncertainties. In this subsection, we examine whether reducing such uncertainties can significantly improve the sensitivity of constraining $\sigma_{\rm wp}$. Fig. 4 shows the effect of statistics on the study of decoherence effect. The y-axis corresponds to the time of data taking. Nevertheless, our simulations suggest that after data collecting for more than 10 years, the limits of $\sigma_{\rm wp}$ are barely improved by collecting more oscillation events.

On the other hand, it is also worthwhile to examine the impact of systematic uncertainties on the study of neutrino wave-packet treatment. Since the wave-packet impact modifies the neutrino oscillation pattern, we believe that the shape uncertainty is the most important uncertainties in the future MBRO experiment(s). Conventionally, the shape uncertainty is assumed to be 1% for all energy bins [20,43,44]. Nevertheless, recently there are literatures suggest that the shape uncertainties could be underestimated. Compared with the conventional prediction, the measured IBD positron (antineutrino) energy spectrum from Daya Bay, Reno and Double Chooz [21–23] show an event excess in the region of 4 to 6 MeV prompt energy. Moreover, the precise shape

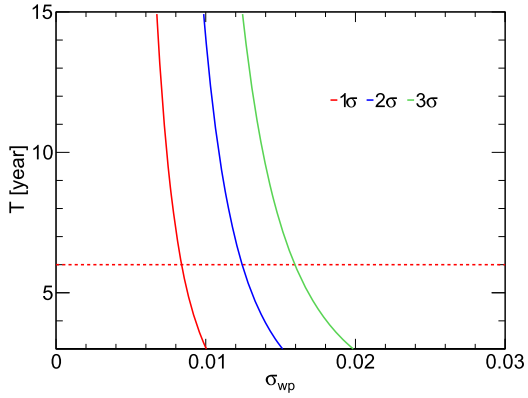

Fig. 4. The sensitivity of constraining $\sigma_{\rm wp}$ vs. years of data taking in the future medium-baseline detector. The horizontal red dashed line represents the nominal running time (six years) proposed in reference [20]. (For interpretation of the colors in the figure(s), the reader is referred to the web version of this article.)

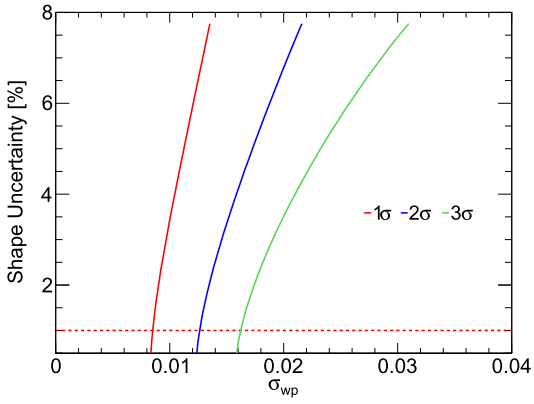

Fig. 5. The sensitivity of constraining $\sigma_{\rm wp}$ vs. shape uncertainties in the future medium-baseline detector. The horizontal red dashed line represents the suggested shape uncertainty (1%) in references [20,43,44].

of the flux spectrum is hard to be determined, which could lead to fine structure and additional shape uncertainties in the analyses of the future MBRO experiment(s) [45–48]. However, we just assume the conventional 1% shape uncertainty in Figs. 3 and 4, which is samed with the References [20,43,44]. To further investigate the impact of shape uncertainty, we alter its values and show the resulting constraint on $\sigma_{\rm wp}$ in Fig. 5.

Fig. 5 shows that the upper bounds on $\sigma_{\rm wp}$ become weaker if shape uncertainty increases, since the observation of decoherence effect or any damping signature depends on the shape analysis. However, the impact of shape uncertainty is not large at all, because as long as the medium-baseline detector manages to resolve multiple neutrino oscillations, the decoherence effect can still be strongly constrained even if the uncertainties of each energy bin become larger. Moreover, our results also suggest that the unknown shape of reactor neutrino flux or issues of potential fine structure [45–48] would not significantly affect the study of neutrino wave-packet impact.

Besides, the detector energy resolution is believed to be more crucial in studying the potential decoherence effect. Fig. 6 shows the importance of detector energy resolution in constraining the

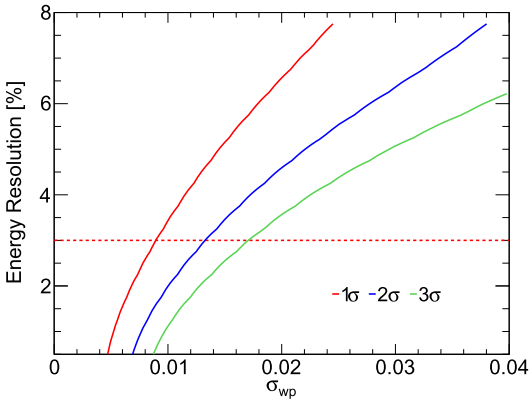

Fig. 6. The sensitivity of constraining $\sigma_{\rm wp}$ vs. detector energy resolution. The horizontal red dashed line represents the proposed (3%) energy resolution of the future MBRO experiment(s) [20].

parameter $\sigma_{\rm wp}$. The red dot-dashed line in this figure represents the results from the proposed detector energy resolution at the future MBRO experiment(s). As a result, the 3 σ C.L. upper bound on $\sigma_{\rm wp}$ is found to be around 0.0162, which is samed with the previous result in Fig. 3.

Comparing Fig. 6 with Figs. 4 and 5, we find that the future MBRO experiment(s) provides an ideal platform for the study on neutrino wave-packet hypothesis and gives rise to the fine upper bounds on the decoherence effect because of the unprecedented detector energy resolution. In addition, improvements on the statistical and systematic uncertainties could further improve the sensitivity, but the effects are not sizable.

3.3. Comparing with the current constraints from Daya Bay

As shown in Fig. 3, the 1, 2, 3 σ C.L. upper bounds on $\sigma_{\rm wp}$ from the future MBRO experiment(s) are 0.0086, 0.0127, 0.0162 respectively. It means that the MBRO experiment(s) can constrain $\sigma_{\rm wp}$ at the order of $O(10^{-2})$, which is around 10 times better than the current results from Daya Bay, thanks to the length of baseline and excellent detector energy resolution of the future MBRO experiment(s). Daya Bay data put an upper limit: $\sigma_{\rm rel} < 0.2$ at 95% C.L.[8] [3], while our simulations suggest that the future MBRO experiment(s) can improve it to $\sigma_{\rm wp} < 0.0125$ at 95% C.L.

On the other hand, regarding to the delocalization effect, the Daya Bay 95% C.L. lower limit is given by:

$$\sigma_{\rm rel} > 2.38 \times 10^{-17} \tag{14}$$

Convert $\sigma_{\rm rel}$ to our definition:

$$\sigma_{\rm wp} > 3.37 \times 10^{-17} \tag{15}$$

[8] Please keep in mind that due to different definition of the width of neutrino wave packet, our $\sigma_{\rm wp}$ is different with the $\sigma_{\rm rel}$ in the Daya Bay paper [3]: $\sigma_{\rm wp} = \sqrt{2}\sigma_{\rm rel}$. Converting to our definition, the Daya Bay 95% C.L. upper bound corresponds to $\sigma_{\rm wp} < 0.283$.

Our simulations suggest that the 1, 2, 3 σ C.L. lower bounds on $\sigma_{\rm wp}$ from the future MBRO experiment(s) are $1.13 \times 10^{-16}, 7.42 \times 10^{-17}, 5.58 \times 10^{-17}$ respectively. The 95% C.L. lower limit is given by:

$$\sigma_{\rm wp} > 7.51 \times 10^{-17}. \tag{16}$$

Our lower limit is larger than the Daya Bay published result, which means that the lower limit of future MBRO experiment(s) is also better than the one of Daya Bay, but the difference is not large. Nevertheless, the practical constraint of $\sigma_x \lesssim O(10)$ m corresponds to $\sigma_{\rm wp} \gtrsim O(10^{-14})$. It implies that both the lower bounds from current and future reactor neutrino experiments are actually weaker than the obvious constraints based on consideration of sizes of reactor cores and detectors. As mentioned before, it is because the delocalization effect is significant only when $\sigma_x \approx L^{\rm osc}$. Therefore, it is expected to be significant only in the oscillations corresponding to $\Delta m^2 \sim 0.1$ eV^2.

4. The potential impact on the precision measurement of θ_{12} and other oscillation parameters

If the decoherence and dispersion effects are significant in MBRO experiment, they could give rise to modification of oscillation patterns and thus affect the identification of the neutrino mass ordering, and also the precision measurements of oscillation parameters. The potential wave-packet impact on the resolution of neutrino mass ordering in MBRO experiment can be found in reference [2]. In this section, we will discuss the wave-packet impact on the measurements of oscillation parameters.

Besides studying the neutrino mass ordering and observations of multiple oscillation cycles, the future MBRO experiment(s) is also expected to provide the unprecedented precision measurements of θ_{12}, Δm^2_{21} and $|\Delta m^2_{ee}|$ to better than 1% [20,49]. Nevertheless, the neutrino wave-packet treatment could potentially lead to the biases on these precision measurements. In order to explore the wave-packet impacts on the future precision measurements, we use Eq. (12), and set $\sigma_{\rm wp}$ and also other oscillation parameters[9] as free parameters in our simulations.

The allowed region of $(\sin^2\theta_{12}, \sigma_{\rm wp})$ is shown in Fig. 7. Our simulations show that the neutrino decoherence barely affect the measurement of θ_{12}. As shown in Fig. 7, larger $\sigma_{\rm wp}$ does not lead to larger value of $\sin^2\theta_{12}$, which ensures unbiased measurement on θ_{12}. Besides, the future MBRO experiment(s) is also expected to provide precision measurements on the solar Δm^2 and atmospheric Δm^2. We also examine the potential neutrino wave-packet impact on the measurements of these two oscillation parameters. The results are shown in Fig. 8. Similarly, these two panels ensure unbiased measurements on $(\Delta m^2_{31} + \Delta m^2_{32})$ / 2 and Δm^2_{21} under neutrino wave-packet treatment.

Our results suggest that although the future MBRO experiment(s) is expected to be more sensitive to the potential wave-packet impact, within the upper bounds of $\sigma_{\rm wp}$, the decoherence and dispersion effects are not large enough to cause significant damping signatures or modifications

[9] According to Reference [2], the decoherence effect could affect the measurements of the oscillation parameters such as the mixing angles and mass square differences. Nevertheless, according to the analysis from Reference [3], the measurement of θ_{13} from Daya Bay is barely affected by the wave-packet impact and the value of $\sin^2 2\theta_{13}$ is not changed. Since Daya Bay is believed to provide the most precise measurement on θ_{13}, in our simulation we use the value of $\sin^2 2\theta_{13}$ as Daya Bay reported and set θ_{13} as a fixed parameter.

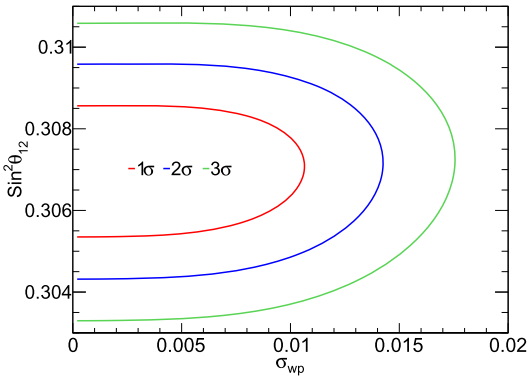

Fig. 7. The 1 σ (red), 2 σ (blue) and 3 σ (green) constraints on "$\sigma_{\rm wp}$ vs $\sin^2\theta_{12}$" for the large $\sigma_{\rm wp}$ region.

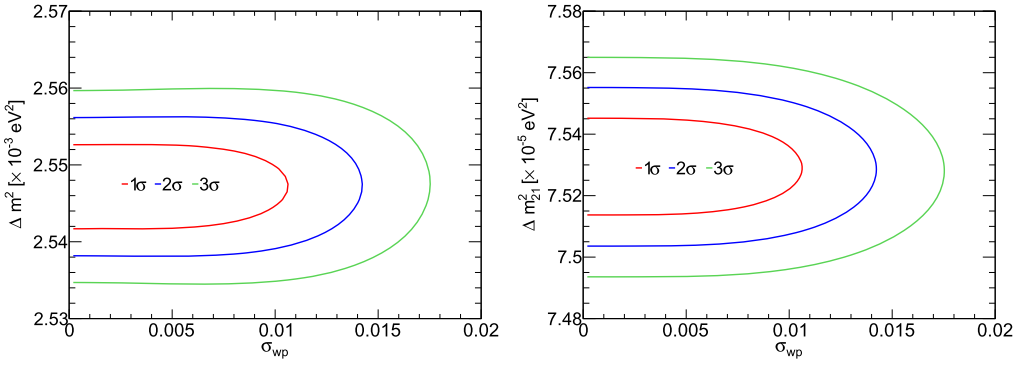

Fig. 8. Left: The 1 σ (red), 2 σ (blue) and 3 σ (green) constraints on "$\sigma_{\rm wp}$ vs Δm^2" for the large $\sigma_{\rm wp}$ region. Right: Same as the left panel, but for "$\sigma_{\rm wp}$ vs Δm^2_{21}".

on the oscillation patterns.[10] Therefore, we believe that the precision measurements on oscillation parameters at future MBRO experiment(s) are extremely safe even if neutrino is treated as wave packet.

5. The proposed extra detector

In section 3, we discussed how the statistical, systematic uncertainties and the resolution affected the sensitivities of MBRO in constraining $\sigma_{\rm wp}$. As a result, the larger statistics, the smaller systematic uncertainty and the nicer energy resolution can always provide a better sensitivity. On the other hand, building an extra detector could also be a potential approach to improvement of the sensitivity. In fact, the JUNO experiment [20] is planning to build a near detector 30-35 m

[10] Recently, we noticed another paper [34] also made a study on constraining the neutrino wave-packet impact in JUNO experiment. Different with our paper, reference [34] constrains the spatial width of the neutrino wave packet (σ_x). The result shows that $\sigma_x > 2.11 \times 10^{-3}$ nm at the 90% C.L., corresponding to $\sigma_{\rm wp} \lesssim O(10^{-2})$. Actually, this result is consistent with our upper limit on $\sigma_{\rm wp}$. Besides, reference [34] also suggests that the precision measurements of θ_{12} and other oscillation parameters are not affected by the potential decoherence effect, which is again consistent with the results of our simulations.

from a European pressure water reactor (EPR) of thermal power 4.6 GW_{th}, JUNO-TAO [50]. In principle, such a small near detector is not sensitive to the decoherence effect since the damping factor in Eq. (4) depends on the baseline L.

However, if an extra detector is built with a baseline of > 10 km, it is expected to be able to improve the constraints on σ_{wp}. Recently, there have been studies [44,51,52] suggest that building an additional detector at the intermediate baseline (around 10 to 40 km) can provide extra sensitivities for the neutrino MH resolution in the future MBRO experiment, since such detector is expected to be able to reduce the correlated uncertainties. Based on the proposal of an extra detector, we further investigate its potential benefits in studying the neutrino wave-packet impact.

5.1. Comparing the sensitivities with single and multiple detectors

We use a similar setup of the extra detector as suggested by Reference [44]: a 4 kton detector with 3% energy resolution, located at baseline of 12.5 km. However, in our simulation, we assume that the extra detector is not identical to the original one and thus will cause uncorrelated uncertainties, which is different with the assumption in Reference [44] and also other literatures [51,52]. We believe that building an identical far and near detector is not feasible because any far detector capable of determining the mass ordering is quite large with a unique geometry, and there will therefore be many uncorrelated uncertainties to deal with. Additionally, if a near detector starts data taking after the far detector, this could introduce additional uncorrelated uncertainties. We believe that the proposed extra detector is not used to cancel the correlated uncertainties such as shape uncertainties. Moreover, as shown in Fig. 5, it is unlikely that the improvements on systematic uncertainties could significantly improve the sensitivity on constraining the parameter σ_{wp}. In our simulations, we not only study the case of correlated shape uncertainties, but also examine the scenario that the shape uncertainties are uncorrelated and cannot be cancelled.

We probe the potential benefits of an additional detector, as Reference [44] suggests that extra detector could give rise to extra sensitivity on the determination of neutrino mass ordering. It is because an intermediate baseline (~ 10 km) detector could provide extra information on the value of Δm^2_{ee} in the analysis, which is important in the neutrino MH resolution. The sensitivity of constraining σ_{wp} with single and multiple detectors is shown in Fig. 9. We compare three different scenarios: single medium-baseline detector (red curve), double detector with correlated (blue curve) and uncorrelated shape uncertainties (magenta curve).

Fig. 9 shows that the proposed extra detector could not significantly improve the sensitivity, no matter the shape uncertainties of two detectors are assumed to be correlated or uncorrelated. The blue curve and magenta curve are close to each other because the shape uncertainties are not crucial in the study of neutrino wave-packet impact, as illustrated in Fig. 5. The tiny difference between red curve and magenta (or blue) curve shows the extra sensitivity provided by the extra detector. Reference [44] suggests that the optimal baseline of extra detector should be around 12.5 km as in such location it could provide largest extra mass ordering sensitivity. However, the optimal location of the extra detector in studying decoherence effect could be different.

5.2. The optimal baseline of the extra detector

In principle, a longer baseline could lead to better sensitivity of σ_{wp}, since the decoherence effect is expected to be more significant at longer distance. However, longer baseline also cor-

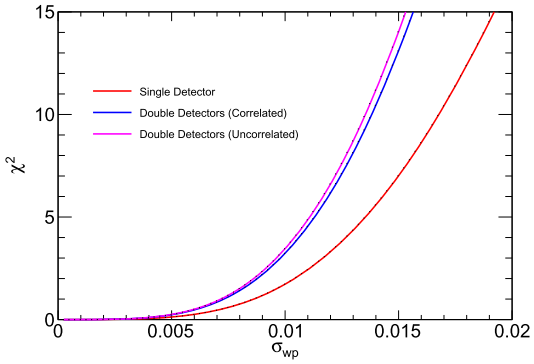

Fig. 9. χ^2 vs $\sigma_{\rm wp}$ for the single and double detector configurations. The red curve reveals the sensitivity of single detector at baseline of 52.5 km; The blue curve represents the case of two detectors, assuming the shape uncertainties are correlated and can be cancelled; The magenta curve corresponds to the assumption that the shape uncertainties are uncorrelated and cannot be canceled.

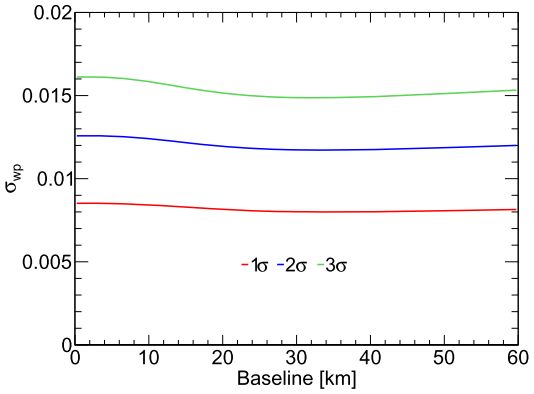

Fig. 10. The 1, 2, 3 σ C.L. upper bound on $\sigma_{\rm wp}$ as a function of baseline of the extra detector.

responds to larger statistical uncertainties. We examine the impact of the baseline on the upper bounds of $\sigma_{\rm wp}$, and search for the optimal location of the extra detector. The results of our numerical simulations are shown in Fig. 10.

According to our simulations, the upper bound on $\sigma_{\rm wp}$ slightly improves as the baseline of the extra detector increases. As mentioned before, longer traveling distance of the neutrinos is expected to enhance the decoherence effect. However, Fig. 10 reveals that the impact of the extra detector is not large. It implies that the sensitivity of constraining $\sigma_{\rm wp}$ is mainly from the original medium-baseline detector, since the corresponding baseline is long and the target mass is large. Changing the location of the 4-ktons extra detector cannot improve the sensitivity of decoherence effect significantly.

6. Conclusion

The neutrino wave-packet impact has been proved to be insignificant in the current reactor neutrino oscillation experiments. However, the plane-wave model of neutrino oscillation is only an approximation, and the wave-packet treatment is more general. Since the future MBRO exper-

iment(s) could resolve multiple neutrino oscillations, it is expected to be an excellent platform to probe the potential decoherence effect or any other damping signatures in neutrino oscillations.

In this article, a wave-packet treatment has been applied to study the $\bar{\nu}_e$ oscillations in the future MBRO experiment(s). The wave-packet treatment (with up to quadratic corrections) leads to decoherence, dispersion and delocalization effects, which modify the neutrino survival probability formula. In this article, numerical simulations for the future MBRO experiment(s) have been performed to probe the potential decoherence and dispersion effects.

Our simulations suggest that the 95% C.L. allowed region of the parameter $\sigma_{\rm wp}$ is given by:

$$7.51 \times 10^{-17} < \sigma_{\rm wp} < 0.0125, \tag{17}$$

which is better than the current constraints from Daya Bay reactor neutrino experiment, especially the upper bound. Moreover, our simulations show that the wave-packet treatment does not lead to significant variations on the oscillation parameters (θ_{12}, Δm^2_{21} and Δm^2_{32}). Within the 3 σ C.L. upper bound of $\sigma_{\rm wp}$, the wave-packet impact is not significant in the future MBRO experiment(s) and does not lead to significant shifts in the best-fit neutrino oscillation parameters.

We also discuss the experimental setups which affect the constraints on the parameter $\sigma_{\rm wp}$. Our simulations show that reducing the statistical uncertainties and shape uncertainties could improve the sensitivity, but the impact is not significant. Similarly, building an extra detector with intermediate baseline ($\sim$ 12 km) could also slightly improve the sensitivity, but the crucial factor is the detector energy resolution.

CRediT authorship contribution statement

Zhaokan Cheng: Formal analysis, Software, Validation, Writing – original draft, Writing – review & editing. **Wei Wang:** Funding acquisition, Methodology, Resources, Supervision, Writing – review & editing. **Chan Fai Wong:** Conceptualization, Funding acquisition, Methodology, Software, Validation. **Jingbo Zhang:** Supervision.

Declaration of competing interest

The authors declare that they have no known competing financial interests or personal relationships that could have appeared to influence the work reported in this paper.

Acknowledgement

The authors thank to Yasaman Farzan, Jiajun Liao, Dmitry Naumov and the JUNO collaboration Speakers Committee for informative discussions and suggestions. This study is supported in part by NSFC grant 11675273 and 2015M582453.

Appendix A. The impact of the input $\sigma_{\rm wp}$ on sensitivity and the measurement of θ_{12}

As mentioned in section 3, we take 10^{-8} as the input value of $\sigma_{\rm wp}$ to produce the measured neutrino events T_i. At the range of $10^{-15} \lesssim \sigma_{\rm wp} \lesssim 10^{-3}$, $\chi^2 \approx 0$ corresponds to the plane-wave limit and the decoherence effects can be safely neglected, as shown in Fig. 3. To make a prudent research, we also attempted to produce the measured neutrino events T_i with observable decoherence effects, such as setting the input value of $\sigma_{\rm wp}$ to be equal to 0.015 or 10^{-16}. The resulting lower and upper bounds are found to be different with the Fig. 3, as shown in the

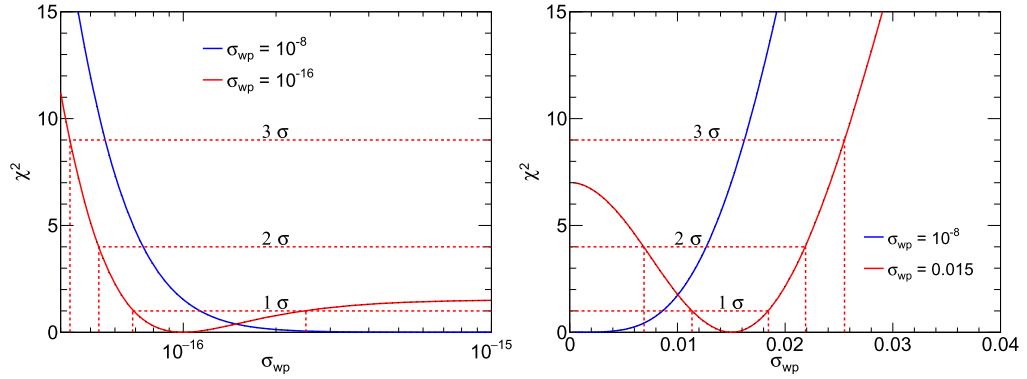

Fig. A.11. Left: the lower bounds on $\sigma_{\rm wp}$ for different assumption of true value of $\sigma_{\rm wp}$ at the future medium-baseline reactor neutrino oscillation experiment(s). Right: the upper bounds on $\sigma_{\rm wp}$. In both panels, the blue curves are same ones in Fig. 3 with assumption of true $\sigma_{\rm wp} = 10^{-8}$. The red solid curves represent the results with the assumptions of true $\sigma_{\rm wp} = 10^{-16}$ and $\sigma_{\rm wp} = 0.015$. The dashed lines show the 1, 2, 3 σ C.L. bounds on $\sigma_{\rm wp}$.

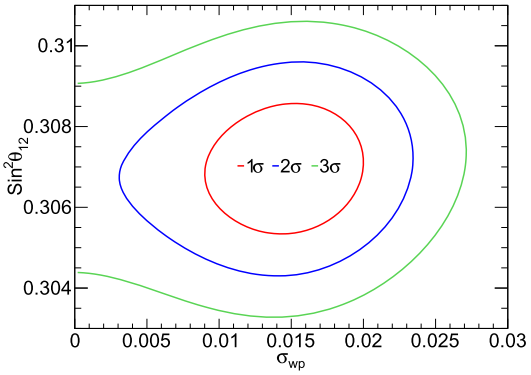

Fig. A.12. The 1 σ (red), 2 σ (blue) and 3 σ (green) constraints on "$\sigma_{\rm wp}$ vs $\sin^2\theta_{12}$" for the large $\sigma_{\rm wp}$ region with assumption of true $\sigma_{\rm wp} = 0.015$.

red curves of Fig. A.11. The left panel shows that the plane-wave hypothesis ($\sigma_{\rm wp} \gtrsim 10^{-15}$) is expected to be ruled out only at around 1 σ C.L., while the right panel reveals that the plane-wave the plane-wave hypothesis ($\sigma_{\rm wp} < 0.001$) can be ruled out at around 2.65 σ (> 99%) C.L.

Compared with Reference [34], Fig. A.11 shows weaker constraints on the decoherence effects. It is because we assume the value of $\sigma_{\rm wp}$ is located in the lower bound and upper bound of the Daya Bay analysis. In Reference [34], the authors would like to study strong decoherence effect and assumed a strong decoherence effect and their input value of σ_x is not within the bound from the Daya Bay analysis [3], as mentioned in their paper. Here, we would like to focus on the range of $\sigma_{\rm wp}$ which is consistent with the Daya Bay data, investigate how can MBRO experiment(s) improves the constraints on relatively weak decoherence effect. Certainly, stronger constraints could be attained if the true value of $\sigma_{\rm wp}$ is found to be beyond the bound from the Daya Bay measurement.

Additionally, we also evaluate the impact of a large input value of $\sigma_{\rm wp}$ on the measurement of θ_{12}. The result is shown in Fig. A.12, which corresponds to setting the input value of $\sigma_{\rm wp}$ as

0.015. As mentioned before, such input value is within the experimental bounds from Daya Bay data, the decoherence effect is actually not too strong. Therefore, the (assumed) decoherence effect does not lead to significant biases on measurement of θ_{12}, as shown in Fig. A.12.

References

[1] S. Eliezer, A.R. Swift, Experimental consequences of electron neutrino-muon-neutrino mixing in neutrino beams, Nucl. Phys. B 105 (1976) 45, https://doi.org/10.1016/0550-3213(76)90059-6.

[2] Y.-L. Chan, M.C. Chu, K.M. Tsui, C.F. Wong, J. Xu, Wave-packet treatment of reactor neutrino oscillation experiments and its implications on determining the neutrino mass hierarchy, Eur. Phys. J. C 76 (6) (2016) 310, https://doi.org/10.1140/epjc/s10052-016-4143-4, arXiv:1507.06421.

[3] F.P. An, et al., Study of the wave packet treatment of neutrino oscillation at Daya Bay, Eur. Phys. J. C 77 (9) (2017) 606, https://doi.org/10.1140/epjc/s10052-017-4970-y, arXiv:1608.01661.

[4] B. Kayser, On the quantum mechanics of neutrino oscillation, Phys. Rev. D 24 (1981) 110, https://doi.org/10.1103/PhysRevD.24.110.

[5] K. Kiers, S. Nussinov, N. Weiss, Coherence effects in neutrino oscillations, Phys. Rev. D 53 (1996) 537–547, https://doi.org/10.1103/PhysRevD.53.537, arXiv:hep-ph/9506271.

[6] C. Giunti, Neutrino wave packets in quantum field theory, J. High Energy Phys. 11 (2002) 017, https://doi.org/10.1088/1126-6708/2002/11/017, arXiv:hep-ph/0205014.

[7] A.D. Dolgov, O.V. Lychkovskiy, A.A. Mamonov, L.B. Okun, M.G. Schepkin, Neutrino wave function and oscillation suppression, Eur. Phys. J. C 44 (2005) 431–434, https://doi.org/10.1140/epjc/s2005-02369-7, arXiv:hep-ph/0506203.

[8] G. Carlo, C.W. Kim, Fundamentals of Neutrino Physics and Astrophysics, Oxford University Press, 2007.

[9] E.K. Akhmedov, A.Y. Smirnov, Paradoxes of neutrino oscillations, Phys. At. Nucl. 72 (2009) 1363–1381, https://doi.org/10.1134/S1063778809080122, arXiv:0905.1903.

[10] D. Naumov, V. Naumov, A diagrammatic treatment of neutrino oscillations, J. Phys. G 37 (2010) 105014, https://doi.org/10.1088/0954-3899/37/10/105014, arXiv:1008.0306.

[11] S. Choubey, S. Petcov, M. Piai, Precision neutrino oscillation physics with an intermediate baseline reactor neutrino experiment, Phys. Rev. D 68 (2003) 113006, https://doi.org/10.1103/PhysRevD.68.113006, arXiv:hep-ph/0306017.

[12] P. Ghoshal, S. Petcov, Addendum: neutrino mass hierarchy determination using reactor antineutrinos, J. High Energy Phys. 1209 (2012) 115, https://doi.org/10.1007/JHEP09(2012)115, arXiv:1208.6473.

[13] L. Zhan, Y. Wang, J. Cao, L. Wen, Determination of the neutrino mass hierarchy at an intermediate baseline, Phys. Rev. D 78 (2008) 111103, https://doi.org/10.1103/PhysRevD.78.111103, arXiv:0807.3203.

[14] L. Zhan, Y. Wang, J. Cao, L. Wen, Experimental requirements to determine the neutrino mass hierarchy using reactor neutrinos, Phys. Rev. D 79 (2009) 073007, https://doi.org/10.1103/PhysRevD.79.073007, arXiv:0901.2976.

[15] X. Qian, D. Dwyer, R. McKeown, P. Vogel, W. Wang, et al., Mass hierarchy resolution in reactor anti-neutrino experiments: parameter degeneracies and detector energy response, Phys. Rev. D 87 (3) (2013) 033005, https://doi.org/10.1103/PhysRevD.87.033005, arXiv:1208.1551.

[16] A. Balantekin, et al., Neutrino mass hierarchy determination and other physics potential of medium-baseline reactor neutrino oscillation experiments, arXiv:1307.7419, 2013.

[17] Y. Takaesu, Determination of the mass hierarchy with medium-baseline reactor-neutrino experiments, arXiv:1304.5306.

[18] Y.F. Li, J. Cao, Y.F. Wang, L. Zhan, Unambiguous determination of the neutrino mass hierarchy using reactor neutrinos, Phys. Rev. D 88 (2013) 013008, https://doi.org/10.1103/PhysRevD.88.013008.

[19] S.-B. Kim, New results from RENO and prospects with RENO-50, Nucl. Part. Phys. Proc. 265–266 (2015) 93–98, https://doi.org/10.1016/j.nuclphysbps.2015.06.024, arXiv:1412.2199.

[20] F. An, et al., Neutrino physics with JUNO, J. Phys. G 43 (3) (2016) 030401, https://doi.org/10.1088/0954-3899/43/3/030401, arXiv:1507.05613.

[21] F. An, et al., Observation of electron-antineutrino disappearance at Daya Bay, Phys. Rev. Lett. 108 (2012) 171803, https://doi.org/10.1103/PhysRevLett.108.171803, arXiv:1203.1669.

[22] J.K. Ahn, et al., Observation of reactor electron antineutrino disappearance in the RENO experiment, Phys. Rev. Lett. 108 (2012) 191802, https://doi.org/10.1103/PhysRevLett.108.191802, arXiv:1204.0626.

[23] Y. Abe, et al., Indication for the disappearance of reactor electron antineutrinos in the double chooz experiment, Phys. Rev. Lett. 108 (2012) 131801, https://doi.org/10.1103/PhysRevLett.108.131801, arXiv:1112.6353.

[24] K. Abe, et al., Observation of electron neutrino appearance in a muon neutrino beam, Phys. Rev. Lett. 112 (2014) 061802, https://doi.org/10.1103/PhysRevLett.112.061802, arXiv:1311.4750.
[25] D. Adey, et al., Measurement of the electron antineutrino oscillation with 1958 days of operation at Daya Bay, Phys. Rev. Lett. 121 (24) (2018) 241805, https://doi.org/10.1103/PhysRevLett.121.241805, arXiv:1809.02261.
[26] M. Beuthe, Oscillations of neutrinos and mesons in quantum field theory, Phys. Rep. 375 (2003) 105–218, https://doi.org/10.1016/S0370-1573(02)00538-0, arXiv:hep-ph/0109119.
[27] M. Blennow, T. Ohlsson, W. Winter, Damping signatures in future neutrino oscillation experiments, J. High Energy Phys. 0506 (2005) 049, https://doi.org/10.1088/1126-6708/2005/06/049, arXiv:hep-ph/0502147.
[28] A.E. Bernardini, M.M. Guzzo, F.R. Torres, Second-order corrections to neutrino two-flavor oscillation parameters in the wave packet approach, Eur. Phys. J. C 48 (2006) 613, https://doi.org/10.1140/epjc/s10052-006-0032-6, arXiv:hep-ph/0612001.
[29] D. Naumov, On the theory of wave packets, Phys. Part. Nucl. Lett. 10 (2013) 642–650, https://doi.org/10.1134/S1547477113070145, arXiv:1309.1717.
[30] A. Chatelain, M.C. Volpe, Neutrino decoherence in presence of strong gravitational fields, Phys. Lett. B 801 (2020) 135150, https://doi.org/10.1016/j.physletb.2019.135150, arXiv:1906.12152.
[31] A.V. Penacchioni, O. Civitarese, Neutrino oscillations and decoherence in short-GRB progenitors, Astrophys. J. 872 (1) (2019) 73, https://doi.org/10.3847/1538-4357/aafe7b, arXiv:1904.07202.
[32] H. Mohammed, J. Evslin, E. Ciuffoli, Measuring entangled neutrino states in a toy model QFT, Nucl. Phys. B 958 (2020) 115113, https://doi.org/10.1016/j.nuclphysb.2020.115113, arXiv:1909.13529.
[33] E. Ciuffoli, J. Evslin, H. Mohammed, Approximate neutrino oscillations in the vacuum, arXiv:2001.03287.
[34] A. de Gouvea, V. de Romeri, C.A. Ternes, Probing neutrino quantum decoherence at reactor experiments, J. High Energy Phys. 08 (2020) 018, https://doi.org/10.1007/JHEP08(2020)049, arXiv:2005.03022.
[35] C. Giunti, Coherence and wave packets in neutrino oscillations, Found. Phys. Lett. 17 (2004) 103–124, https://doi.org/10.1023/B:FOPL.0000019651.53280.31, arXiv:hep-ph/0302026.
[36] C. Fuji, Y. Matsuura, T. Shibuya, S. Tsai, A wave-packet view of neutrino oscillation and pion decay, arXiv:hep-ph/0612300.
[37] C. Kim, Neutrino physics: fundamentals of neutrino oscillations, arXiv:hep-ph/9607391.
[38] E. Akhmedov, D. Hernandez, A. Smirnov, Neutrino production coherence and oscillation experiments, J. High Energy Phys. 1204 (2012) 052, https://doi.org/10.1007/JHEP04(2012)052, arXiv:1201.4128.
[39] D. Hernandez, A.Yu. Smirnov, Active to sterile neutrino oscillations: coherence and MINOS results, Phys. Lett. B 706 (2012) 360–366, https://doi.org/10.1016/j.physletb.2011.11.031, arXiv:1105.5946.
[40] J. Rich, The quantum mechanics of neutrino oscillations, Phys. Rev. D 48 (1993) 4318–4325, https://doi.org/10.1103/PhysRevD.48.4318.
[41] W. Grimus, P. Stockinger, Real oscillations of virtual neutrinos, Phys. Rev. D 54 (1996) 3414–3419, https://doi.org/10.1103/PhysRevD.54.3414, arXiv:hep-ph/9603430.
[42] M. Tanabashi, et al., Review of particle physics, Phys. Rev. D 98 (3) (2018) 030001, https://doi.org/10.1103/PhysRevD.98.030001.
[43] Y.-F. Li, J. Cao, Y. Wang, L. Zhan, Unambiguous determination of the neutrino mass hierarchy using reactor neutrinos, Phys. Rev. D 88 (1) (2013) 013008, https://doi.org/10.1103/PhysRevD.88.013008, arXiv:1303.6733.
[44] H. Wang, L. Zhan, Y.-F. Li, G. Cao, S. Chen, Mass hierarchy sensitivity of medium baseline reactor neutrino experiments with multiple detectors, Nucl. Phys. B 918 (2017) 245–256, https://doi.org/10.1016/j.nuclphysb.2017.03.002, arXiv:1602.04442.
[45] D.A. Dwyer, T.J. Langford, Spectral structure of electron antineutrinos from nuclear reactors, Phys. Rev. Lett. 114 (1) (2015) 012502, https://doi.org/10.1103/PhysRevLett.114.012502, arXiv:1407.1281.
[46] A.A. Sonzogni, M. Nino, E.A. McCutchan, Revealing fine structure in the antineutrino spectra from a nuclear reactor, Phys. Rev. C 98 (1) (2018) 014323, https://doi.org/10.1103/PhysRevC.98.014323, arXiv:1710.00092.
[47] F. Capozzi, E. Lisi, A. Marrone, Neutrino mass hierarchy and precision physics with medium-baseline reactors: impact of energy-scale and flux-shape uncertainties, Phys. Rev. D 92 (9) (2015) 093011, https://doi.org/10.1103/PhysRevD.92.093011, arXiv:1508.01392.
[48] Z. Cheng, N. Raper, W. Wang, C.F. Wong, J. Zhang, Potential impact of sub-structure on the resolution of neutrino mass hierarchy at medium-baseline reactor neutrino oscillation experiments, arXiv:2004.11659.
[49] L.J.W.J. Cao, Y.F. Wang, Reactor neutrino experiments: present and future, Annu. Rev. Nucl. Part. Sci. 67 (2017) 183–211, https://doi.org/10.1146/annurev-nucl-101916-123318, arXiv:1803.10162.
[50] G.C. (on behalf of JUNO), JUNO-TAO experiment with large area high performance SiPMs, in: SiPM Workshop: From Fundamental Research to Industrial Applications, 2019.

[51] E. Ciuffoli, J. Evslin, Z. Wang, C. Yang, X. Zhang, W. Zhong, Medium baseline reactor neutrino experiments with two identical detectors, Phys. Lett. B 736 (2014) 110–118, https://doi.org/10.1016/j.physletb.2014.07.007, arXiv:1211.6818.

[52] E. Ciuffoli, J. Evslin, Z. Wang, C. Yang, X. Zhang, et al., Advantages of multiple detectors for the neutrino mass hierarchy determination at reactor experiments, Phys. Rev. D 89 (2014) 073006, https://doi.org/10.1103/PhysRevD.89.073006, arXiv:1308.0591.